J Mater Sci (2008) 43:425–433
DOI 10.1007/s10853-007-1929-7

Effect of alpha prime due to 475 °C aging on fracture behavior and corrosion resistance of DIN 1.4575 and MA 956 high performance ferritic stainless steels

Maysa Terada · Marcio F. Hupalo · Isolda Costa · Angelo F. Padilha

Received: 26 December 2006 / Accepted: 8 June 2007 / Published online: 15 November 2007

Abstract The 475 °C embrittlement in stainless steels is a well-known phenomenon associated to alpha prime (α') formed by precipitation or spinodal decomposition. Many doubts still remain on the mechanism of α' formation and its consequence on deformation and fracture mechanisms and corrosion resistance. In this investigation, the fracture behavior and corrosion resistance of two high performance ferritic stainless steels were investigated: a superferritic DIN 1.4575 and MA 956 superalloy were evaluated. Samples of both stainless steels (SS) were aged at 475 °C for periods varying from 1 to 1,080 h. Their fracture surfaces were observed using scanning electron microscopy (SEM) and the cleavage planes were determined by electron backscattering diffraction (EBSD). Some samples were tested for corrosion resistance using electrochemical impedance spectroscopy (EIS) and potentiodynamic polarization. Brittle and ductile fractures were observed in both ferritic stainless steels after aging at 475 °C. For aging periods longer than 500 h, the ductile fracture regions completely disappeared. The cleavage plane in the DIN 1.4575 samples aged at 475 °C for 1,080 h was mainly {110}, however the {102}, {314}, and {131} families of planes were also detected. The pitting corrosion resistance decreased with aging at 475 °C. The effect of alpha prime on the corrosion resistance was more significant in the DIN 1.4575 SS comparatively to the Incoloy MA 956.

M. Terada (✉) · I. Costa
Instituto de Pesquisas Energéticas e Nucleares, CCTM, Av. Lineu Prestes, 2242, Cidade Universitária, Butantã, CEP 05508-900 Sao Paulo, SP, Brazil
e-mail: maysaterada@uol.com.br

M. F. Hupalo
Sociedade Educacional de Santa Catarina, Instituto Superior Tupy, Rua Albano Schmidt, 3333, Boa Vista, CEP 89227-700 Joinville, SC, Brazil

A. F. Padilha
Depto de Engenharia Metalúrgica e de Materiais, Escola Politécnica da Universidade de São Paulo, Av. Prof. Mello Moraes, 2463, Cidade Universitária, Butantã, CEP 05508-030 Sao Paulo, SP, Brazil

Introduction

The 475 °C embrittlement occurs in most of the ferritic or duplex stainless steels aged in a temperature from 300 to 550 °C [1] and it is caused by alpha prime (α') formed in the ferrite phase by a nucleation and growth precipitation process or by spinodal decomposition. Alpha prime is rich in chromium and iron and its structure is body centered cubic (BCC). Its presence results in loss of properties such as ductility, toughness, and corrosion resistance. This phenomenon has been well known for more than 60 years. However, many doubts still remain on the mechanism of α' formation and its consequence on deformation and fracture mechanisms [2, 3]. Long aging times result not only in increased hardness and mechanical strength but also affect their corrosion resistance. It has been shown that depending on the amount of α' in the alloy, its pitting corrosion resistance might significantly decrease [4].

The consequences of aging at 400 and 475 °C on the mechanical properties and corrosion behavior of the ferritic stainless steel AISI 444 (18Cr-2Mo-type) were investigated by Souza et al. [5]. The age hardening was more severe at 475 °C and the susceptibility to localized corrosion increased, while the impact toughness decreased with aging time.

The yield stress and tensile strength increase with aging time [4]. The fracture behavior of the stainless steel, which is usually ductile, showing typical wavy deformation lines and dimples, after the α' formation becomes brittle, presenting straight deformation lines and cleavage, increasing the ductile-brittle transition temperature [6]. The incidence of α' also hinders dislocations movement, causing straight deformation lines, and even twin boundaries [7].

The fracture mechanism in 475 °C embrittled ferritic stainless steels E-Brite (26Cr type) and AL29-4 (29Cr-4Mo-type) was investigated by Marrow [8] and deformation twinning occurrence during brittle fracture was detected.

Decomposition mechanism and embrittlement during aging at 475 °C in an experimental ferritic stainless steel containing 38 wt.% chromium were studied by Cortie and Pollack [9]. The hardness was strongly affected by alpha prime formation, but the toughness seems to be controlled by processes, such as dislocation pinning by chromium, carbon, and nitrogen atoms, that occurred previous to significant spinodal decomposition.

González-Carrasco et al. [10] studied the corrosion behavior of MA 956 after 475 °C aging and found that the uniform corrosion was independent of the material state. On the other hand, the pitting corrosion resistance was strongly affected by the degree of α' formation.

In this investigation, two high performance ferritic stainless steels, specifically DIN 1.4575 and Incoloy MA 956 were aged at 475 °C for periods varying in the range from 1 to 2,348 h. After aging heat treatments, some samples were analyzed using transmission electron microscopy (TEM). Besides, some samples were observed by scanning electron microscopy (SEM), after being fractured. The cleavage planes were determined using electron backscattering diffraction (EBSD) technique. The corrosion resistance of both steels after the various aging heat treatments was also investigated by electrochemical impedance spectroscopy (EIS) and potentiodynamic polarization curves.

Experimental

Table 1 shows the chemical composition (wt.%) of DIN 1.4575 and Incoloy MA 956. The DIN 1.4575 samples were solution annealed at 1,050 °C for 30 min and the Incoloy MA 956, at 1,200 °C for 60 min (1 h).

After the solution annealing, the samples were aged at 475 °C for periods varying from 1 to 2,348 h, as shown in Table 2 and then some were observed using TEM and others were V-notched as illustrated in Fig. 1, fractured and analyzed by SEM and EBSD. The crack propagation was studied on the X-surface.

Table 1 Chemical composition (wt.%) of DIN 1.4575 and Incoloy MA 956 stainless steels [6]

	DIN 1.4575	Incoloy MA 956
Al	–	5.51
C	0.01	0.017
Co	0.02	0.11
Cr	28.12	21.26
Cu	0.04	0.11
Mn	0.22	0.143
Mo	2.44	0.156
N	0.011	–
Nb	0.31	0.027
Ni	3.91	0.088
P	0.014	0.015
S	0.003	0.03
Si	0.35	0.074
Ti	0.01	0.372
V	0.05	0.057
W	0.02	–
Y_2O_3	–	0.42

Table 2 Aging time at 475 °C for DIN 1.4575 (solution annealed at 1,050 °C for 30 min) and Incoloy MA 956 (solution annealed at 1,200 °C for 60 min) samples

Sample	DIN 1.4575 (h)	Incoloy MA 956 (h)
1	1	1
2	150	150
3	317	317
4	648	648
5	811	738
6	1,080	2,348

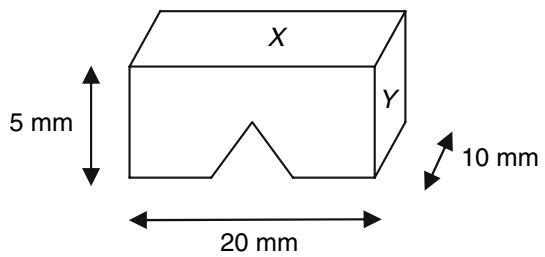

Fig. 1 Schematic illustration of sample used for fracture tests. X is the metallographically prepared surface. Y is the surface where the compression force was applied

Some of the aged samples had their corrosion properties analyzed by electrochemical methods. For this evaluation all specimens were ground up to #600 with silicon carbide paper, and then rinsed with demonized water, degreased

Table 3 Composition of PBS solution

NaCl	8.77 g/L
Na_2HPO_4	1.42 g/L
KH_2PO_4	2.72 g/L
pH	7

with acetone and immersed in a phosphate buffered solution (PBS) at room temperature for 24 h prior to the electrochemical measurements. The composition of the PBS solution is given in Table 3.

The electrochemical tests were performed using a three-electrode cell set-up, with a platinum wire and a saturated calomel electrode (SCE) as counter and reference electrodes, respectively. EIS measurements were accomplished using a 1255 Solartron frequency response analyzer coupled to an EG&G 273A potentiostat. All EIS measurements were obtained in the potentiostatic mode at the open-circuit potential (OCP). The amplitude of the signal was 10 mV and the investigated frequency was from 100 kHz to 10 mHz with an acquisition rate of 6 points per decade. After the EIS tests, potentiodynamic polarization measurements were obtained in the range from the OCP up to 1,200 mV at a scan rate of 1 mV s^{-1}. From the polarization curves, the values of passive film breakdown potential were obtained. After polarization tests, the pits morphologies were observed by SEM using a Philips XL30 microscope.

Results and discussion

The variation of hardness with aging time (see Fig. 2) gives a general overview of alpha prime formation kinetics in both investigated alloys. It clearly shows that the superferritic steel DIN 1.4575 is more prone to alpha prime formation than the MA 956 superalloy. The magnitude of the alpha prime (α') effects on the alloy properties depends chiefly on the alloy chromium content and it increases with chromium content. For instance, in alloys with 25–30 wt.% chromium, long aging at temperatures around 475 °C might increase two-fold its hardness [2, 11]. Its maximum hardness may reach values higher than 350 HV. In alloys containing 21 wt.% chromium, the increase in maximum hardness was about 80% and the value reached was 298 HV [7]. For alloys with 18 wt.% chromium, the maximum harness increase was about 50% [1, 2, 12].

Despite the low contrast and small size of the alpha prime, usually between 20 and 200 Å, and its high resistance to coalesce, alpha prime was observed by TEM at the grain boundaries and inside the grains of DIN 1.4575 steel aged for 811 h, Fig. 3. In this particular case, the alpha prime size was between 50 and 300 Å. The MA 956 alloy was not investigated by TEM.

The solution annealed samples presented ductile fracture, as shown in Fig. 4a (DIN 1.4575). Alpha prime clusters that block dislocations movements, diminishing the number of active slip planes inside the material, cause embrittlement [6–8]. Brittle fracture was also seen at some

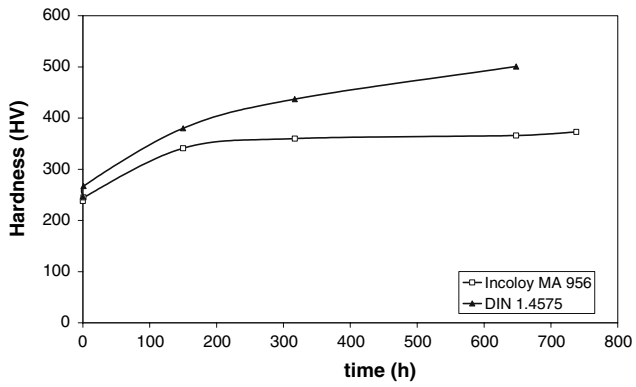

Fig. 2 Effect of alpha prime in the Vickers Hardness of DIN 1.4575 and MA 956

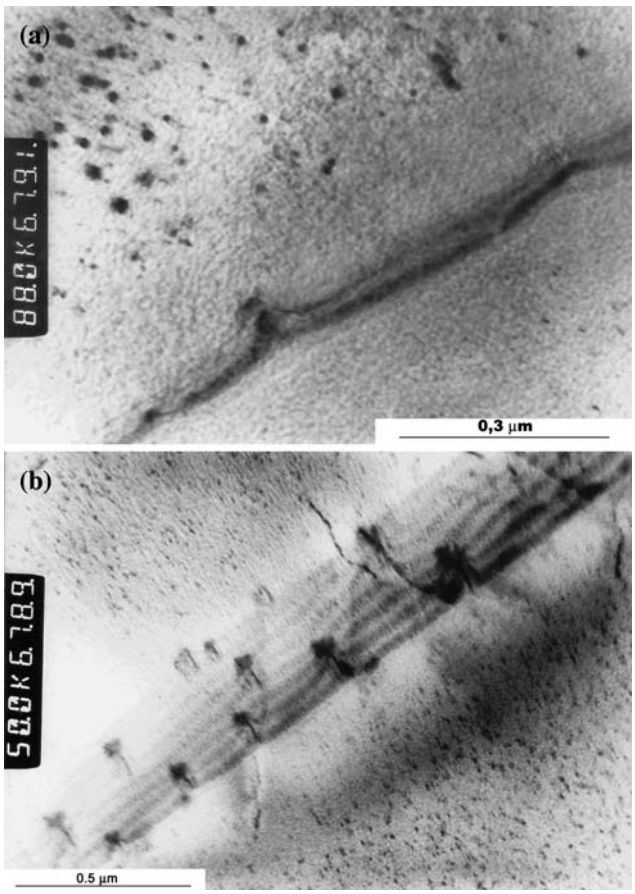

Fig. 3 TEM micrographs of DIN 1.4575 annealed and aged at 475 °C for 811 h showing alpha prime (**a**) inside the grains and (**b**) at grain boundary

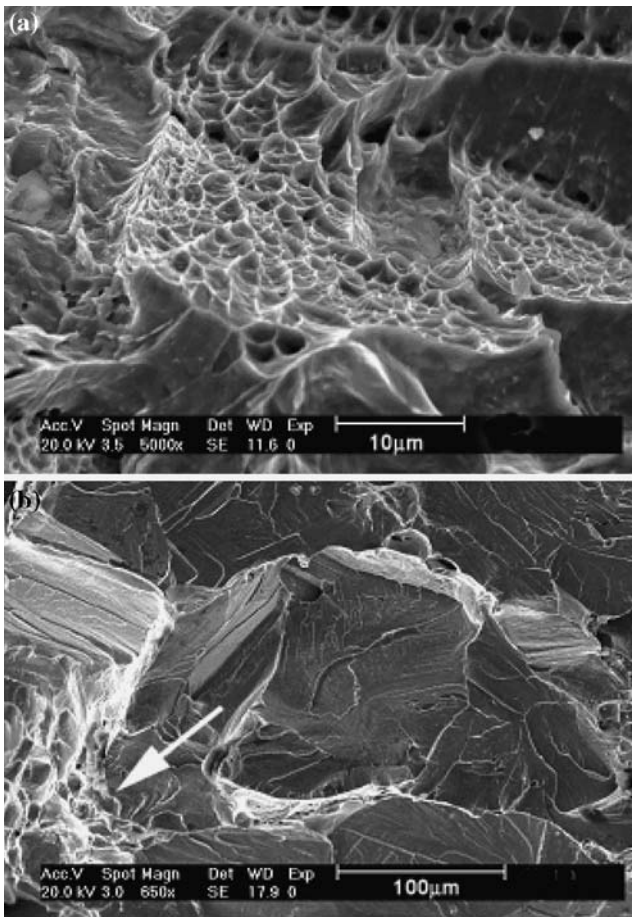

Fig. 4 SEM micrographs of fractured area in DIN 1.4575 samples (**a**) Ductile fracture typical of the annealed sample. (**b**) Brittle and ductile fracture (pointed by arrow) in 1-h aged (475 °C) sample

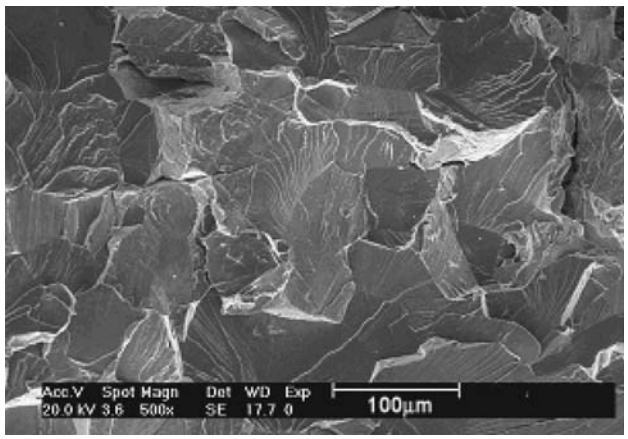

Fig. 5 Brittle fracture in DIN 1.4575 sample aged for 1,080 h (45 days) at 475 °C

areas of the 1-h aged DIN 1.4575 steel, as shown in Fig. 4b. For 500-h aging samples, brittle fracture was predominant, as Fig. 5 shows, and twin boundaries, instead

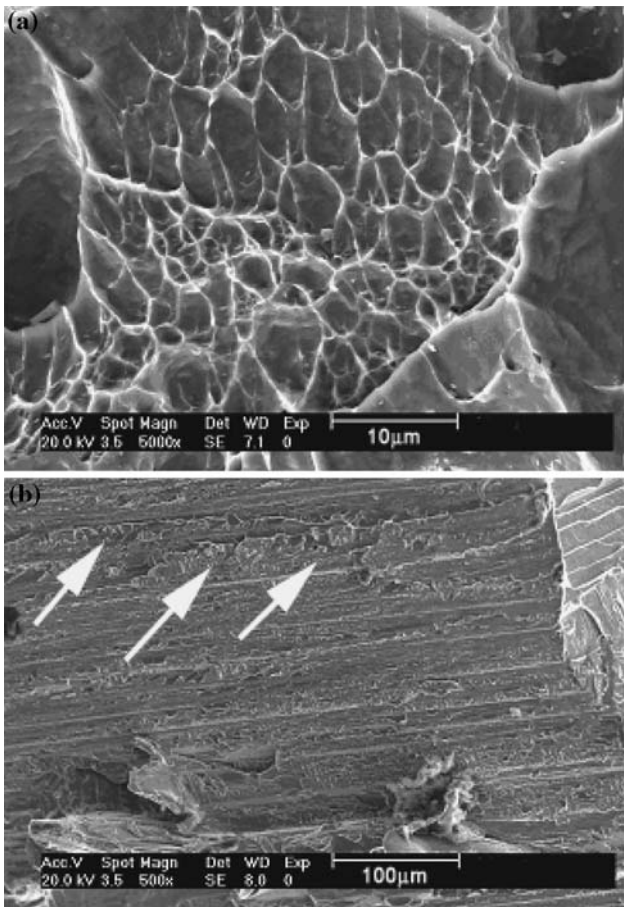

Fig. 6 SEM micrography of fractured MA 956 samples (**a**) Ductile fracture typical of annealed ferrite. (**b**) Brittle and ductile fracture (pointed by arrows) in sample aged at 475 °C for 10 h

of the wavy deformation lines typical of ductile ferritic microstructure, were seen. Similar behavior was associated to the MA 956 steel, with solution annealed samples presenting ductile fracture, as shown in Fig. 6a, but brittle fracture being predominant for samples after 10-h aging (Fig. 6b).

Figure 6a exemplifies the typical ductile stainless steel fracture, and Fig. 6b, the cleavage fracture caused by α' formation. Figure 7 shows fracture surfaces of Incoloy MA 956 samples solution annealed and aged at 475 °C for 738 h. Analysis of the fractured samples shows that the longer the aging time, more brittle is the steel [6].

The orientation of the cleavage fractures in the DIN 1.4575 aged at 475 °C for 1,080 h was determined using the EBSD technique and it was mainly at family {110}. The {102}, {314}, and {131} families of planes were also observed. According to literature, the cleavage fracture in ferritic stainless steels is usually at {100} family of planes, although there are also examples for which the {110} cleavage planes are preferred [13–15].

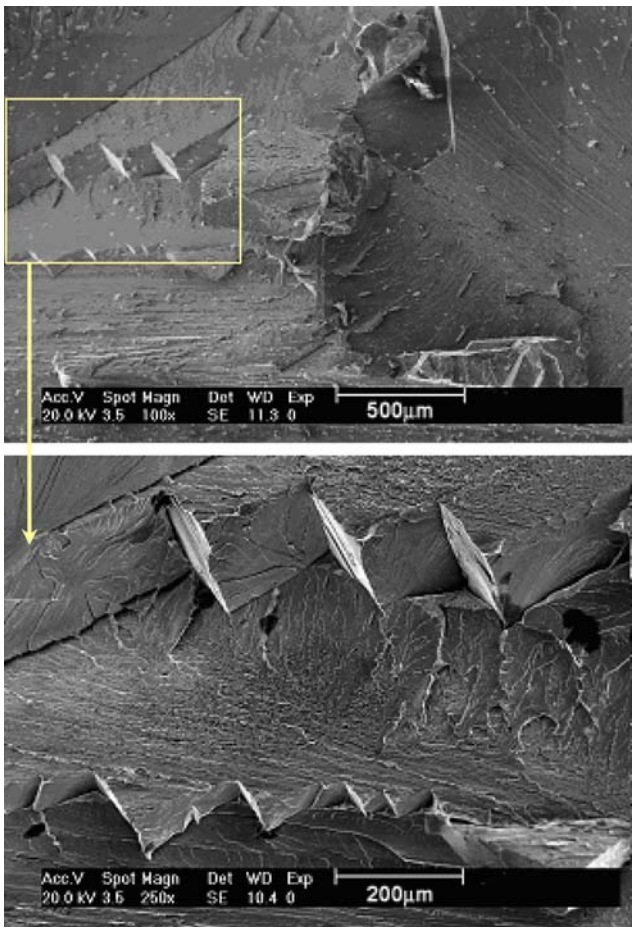

Fig. 7 Cleavage fracture of the Incoloy MA 956 aged at 475 °C for 738 h

The corrosion resistance of some of the aged samples was studied by EIS and the results are presented in Fig. 8. The Nyquist diagrams show that the impedance decreased with aging time. The Bode diagrams for the solution annealed samples show a large plateau at high phase angles (approximately –80°) at low frequencies, typical of passive materials. For the DIN 1.4575 aged samples, the phase angle at low frequencies decreased with aging time, suggesting the decrease in the corrosion resistance. The large plateau at low frequencies also indicates the interaction of more than one time constant.

Figure 9 shows the potentiodynamic polarization curves obtained for some of the aged samples and the corresponding breakdown potentials are presented in Table 4. After the polarization tests, the surface of the polarized samples was observed by SEM. The results showed that pits density and depth increased with aging time (see Fig. 10).

For the Incoloy MA 956 samples, the EIS diagrams (Fig. 11) revealed that alpha prime did not considerably affect their electrochemical behavior. In fact, the results showed that the impedance of the samples aged for 317 h increased in comparison to the solution annealed ones. The literature suggests that the high corrosion resistance of this type of alloys is associated to the aluminum oxide on the alloy surface [5]. A thicker oxide film is expected on the samples aged for 317 h comparatively to the solution annealed ones. However, for longer aging periods, the impedance continuously decreased, Fig. 11. It is possible that for long aging periods the beneficial effect of the aluminum oxide film is counterbalanced by the increasing harmful effects of the alpha prime.

Comparison of all the EIS diagrams suggests that the effect of aging time is more significant on the corrosion resistance of the MA 956 steel than on the DIN 1.4575 one. The results also indicate that the oxide layer on the first steel is more stable than on the last one. This could be due to the presence of aluminum in the MA 956 steel favoring the formation of a more protective layer on its surface.

Potentiodynamic polarization curves for the MA 956 samples are shown in Fig. 12 and the corrosion and breakdown potentials obtained from these curves are given in Table 5. The results confirm the detrimental influence of alpha prime on the localized corrosion resistance of the alloy showing the decrease in the breakdown potential with aging time. A comparison of the breakdown potentials of the two steels aged for a same period of time (648 h) show lower values associated to the MA 956 as compared to the 1.4575 steel. This could be due to the lower chromium contents in the MA 956 steel and indicates that for localized corrosion resistance higher chromium contents would be advantageous. The alpha prime is a Cr rich phase and its formation leads to Cr impoverishment in the matrix resulting in local action cells and consequently to pitting initiation. This usually initiates by halide ions adsorption, in the electrolyte used specifically chloride ions, on the defective regions of the oxide film, such as the areas with low chromium content where the oxide film would be less protective. After the pit has nucleated it might either repassivate or autocatalytically propagate by any or both mechanisms, active-passive cell and differential aeration cell.

The SEM micrographs of the MA 956 solution annealed steel after polarization tests showed only one pit on each polarized sample, Fig. 13, indicating that the propagation of only one pit is enough to cause film breakdown. However, for the MA 956 steel aged for 317 h two pits were seen, although they were of smaller size than that on the solution annealed one. The number of pits increased with aging time, and also their depth and width increased, as shown in Fig. 13c and d, supporting the deleterious

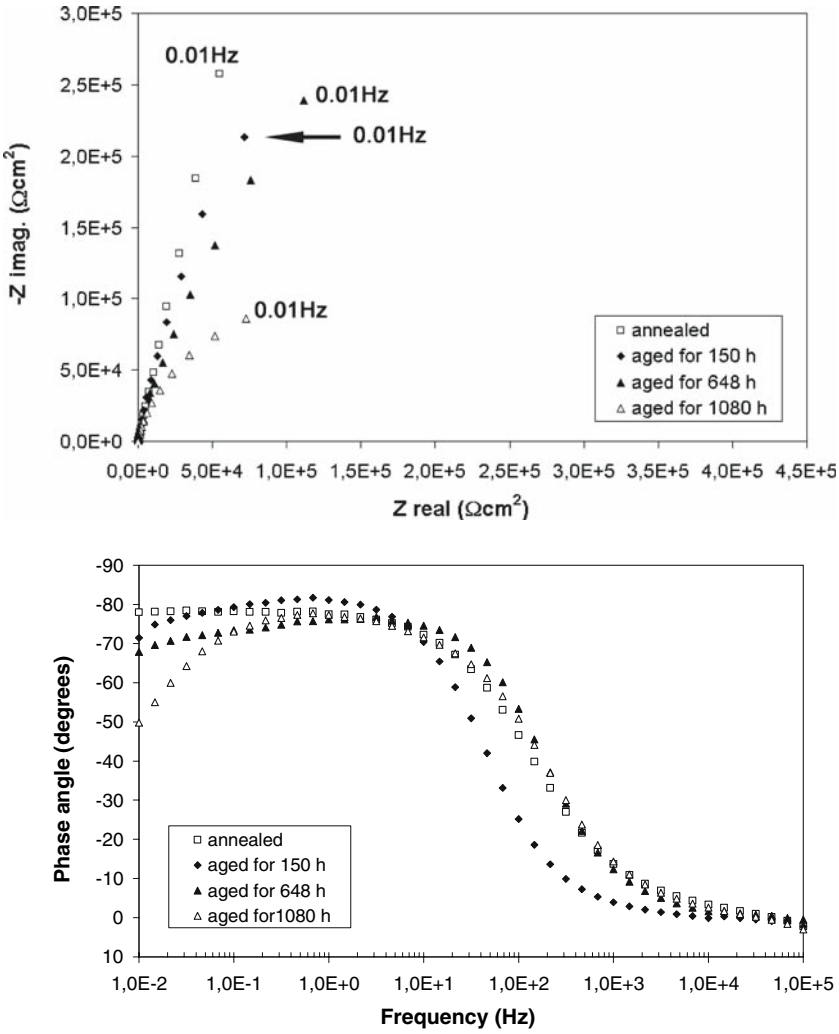

Fig. 8 EIS diagrams obtained for DIN 1.4575 annealed and aged at 150, 648, and 1,080 h. EIS tests were carried out after 24 h of immersion in PBS solution at 25 °C

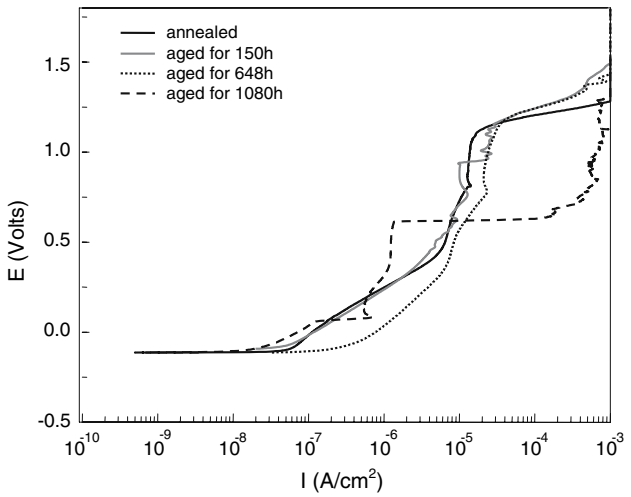

Fig. 9 Potentiodynamic polarization curves for DIN 1.4575 steel annealed and aged for various periods. Results obtained after 24 h of immersion in PBS solution at 25 °C

Table 4 Breakdown potential values for DIN 1.4575 solution annealed and aged at 475 °C for 150, 648, and 1,080 h

Sample	*E* (V/SCE)
Solution annealed	1.10
Aged for 150 h	0.92
Aged for 648 h	0.78
Aged for 1,080 h	0.6

effect of alpha prime on the localized corrosion resistance of the ferritic stainless steels investigated.

The results suggest that α' was responsible for the embrittlement and for the corrosion resistance decrease of both tested stainless steels, DIN 1.4575 and Incoloy MA 956. The results of EIE and potentiodynamic polarization tests confirm that the presence of alpha prime reduces the localized corrosion resistance [5, 10] of both materials.

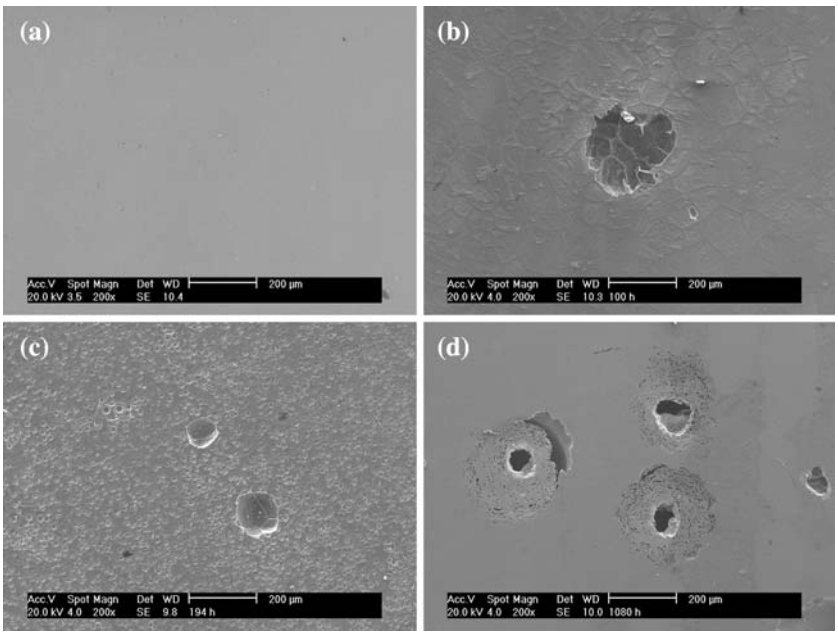

Fig. 10 SEM micrographs of DIN W. 1.4575 after polarization tests. Solution annealed samples (**a**); and annealed and aged at 475 °C for 100 h (**b**); 194 h (**c**); and 1,080 h (**d**)

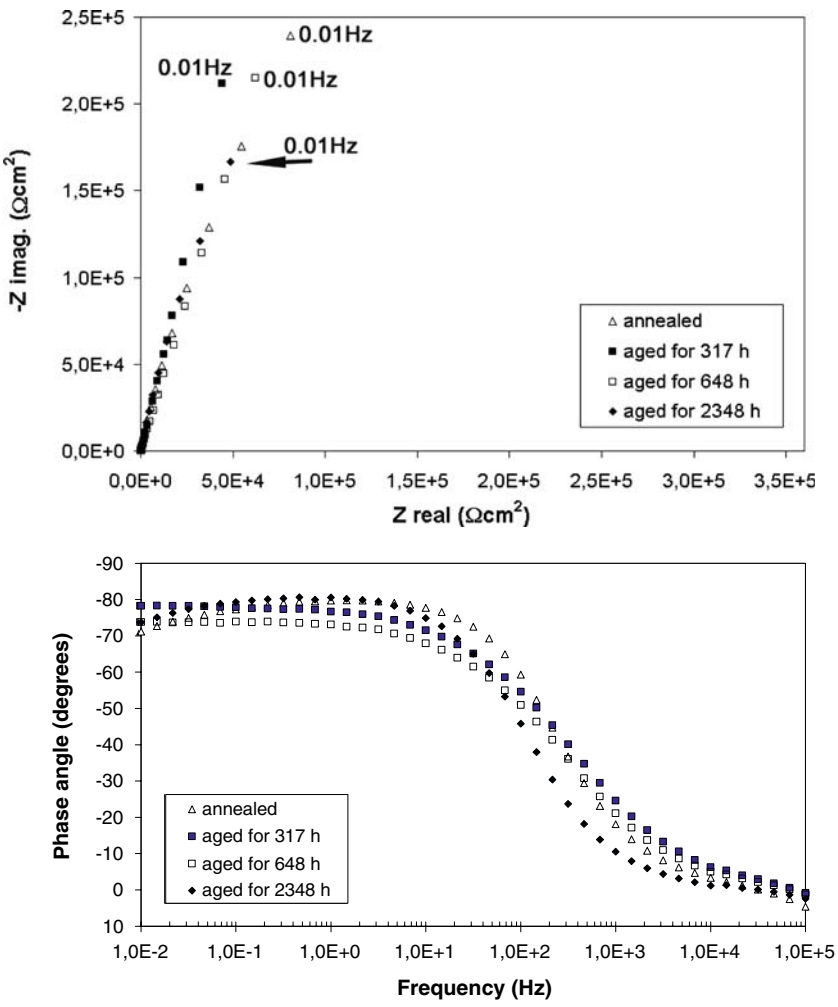

Fig. 11 EIS diagrams obtained for MA 956 annealed and aged at 150, 648 and 1,080 h. Results obtained after 24 h of immersion in PBS solution at 25 °C

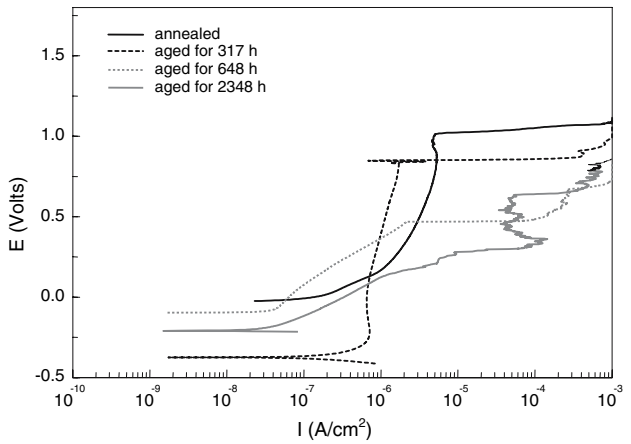

Fig. 12 Potentiodynamic polarization curves for MA 956 steel annealed and aged for various periods. Tests were carried out after 24 h of immersion in PBS solution at 25 °C

Conclusions

The results of the present study showed that both tested steels, superferritic DIN 1.4575 and Incoloy MA 956, were highly susceptible to alpha prime formation at 475 °C. Despite its low contrast and small size (50–300 Å), alpha prime was detected by TEM. As expected, the consequences of aging at 475 °C on the mechanical properties and corrosion behavior increased with time of aging. Ductile fractures and cleavage regions were found in both ferritic stainless steels tested after aging. For aging periods longer than 500 h, the ductile fracture areas (dimples) completely disappeared. The cleavage planes for DIN 1.4575 aged at 475 °C for 1,080 h were mainly {110}, however the {102}, {314}, and {131} families of planes were also detected.

Table 5 Breakdown potential values for MA 956 solution annealed and aged at 475 °C for 317, 648, and 2,348 h

	E (V/SCE)
Solution annealed	1.0
Aged for 317 h	0.77
Aged for 648 h	0.46
Aged for 2,348 h	0.21

The pitting corrosion resistance of the tested steels decreased with aging time and the effect of alpha prime on the steel localized corrosion resistance was more significant for the MA 956 comparatively to the DIN 1.4575 one, likely due to the lower chromium content in the MA 956 steel. On the other hand, the oxide film on this last steel was more stable under undisturbed conditions, suggesting that Al addition improves the film properties at the corrosion potential.

The main conclusion of the present study is that the DIN 1.4575 is more susceptible to alpha prime formation and consequently to loss of toughness than the superalloy MA 956, confirming that the chromium content of the alloy has a major effect on the alpha prime susceptibility of the alloy.

Acknowledgements The authors acknowledge FAPESP, CNPq and CAPES for financial support. Dr. Clarice T. Kunioshi is also acknowledged for the SEM micrographs.

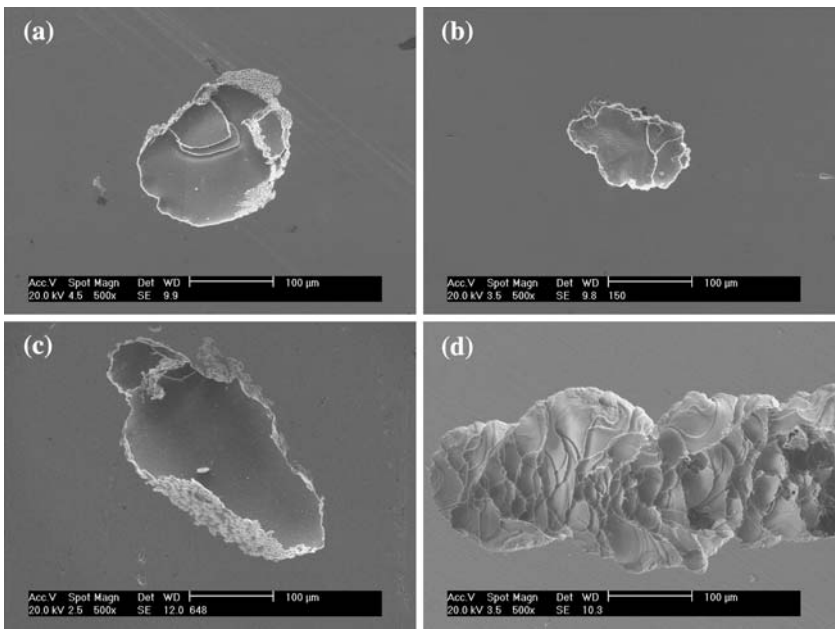

Fig. 13 SEM micrographs of Incoloy MA 956 after polarization tests. Annealed (**a**) and annealed and aged at 475 °C for 150 h (**b**); 648 h (**c**); and 738 h (**d**)

References

1. Grobner PJ, Steigerwald RF (1977) JOM 29:17
2. Bandel G, Tofaute W (1942) Arch Eisenhüttenwes 14:307
3. Rechemberg HR, Brandi SD, Padilha AF (1994) In: 48th Congresso Anual da ABM, São Paulo, Brazil, p 477 (In Portuguese)
4. Ura MM, Padilha AF, Alonso N (1995) In: 49th Congresso Anual da ABM, São Paulo, Brazil, p 337 (In Portuguese)
5. Souza JA, Abreu HFG, Nascimento AM, De Paiva JAC, De Lima-Neto P, Tavares SSM (2005) J Mater Eng Perf 14:367
6. Terada M (2003) MSc. Dissertation. Escola Politécnica da Universidade de São Paulo, 94 p (In Portuguese)
7. Blackburn MJ, Nutting J (1964) J Iron Steel I 202:610
8. Marrow TJ (1996) Fatigue Fract Eng Mater Struct 19:919
9. Cortie MB, Pollack H (1995) Mater Sci Eng A 199:153
10. González-Carrasco JL, Escudero ML, Martín FJ, García-Alonso MC, Chao J (2001) Corros Sci 43:1081
11. Newel HD (1946) Metal Prog 50:997–1006, and 1016–1028
12. Jacobsson P, Bergström Y, Aronsson B (1975) Metall Trans 6A:1577
13. Barrett CS, Bakish R (1958) Trans Metall Soc AIME 212:122
14. Davies PA, Randle V (2001) J Microsc Oxford 204:29
15. Davies PA, Novovic M, Randle V, Bowen P (2002) J Microsc Oxford 205:278